LETTER

doi:10.1038/nature12321

Mitotic trigger waves and the spatial coordination of the *Xenopus* cell cycle

Jeremy B. Chang[1] & James E. Ferrell Jr[1,2]

Despite the large size of the *Xenopus laevis* egg (approximately 1.2 mm diameter), a fertilized egg rapidly proceeds through mitosis in a spatially coordinated fashion. Mitosis is initiated by a bistable system of regulatory proteins centred on Cdk1 (refs 1, 2), raising the possibility that this spatial coordination could be achieved through trigger waves of Cdk1 activity[3]. Using an extract system that performs cell cycles *in vitro*, here we show that mitosis does spread through *Xenopus* cytoplasm via trigger waves, propagating at a linear speed of approximately 60 μm min^{-1}. Perturbing the feedback loops that give rise to the bistability of Cdk1 changes the speed and dynamics of the waves. Time-lapse imaging of intact eggs argues that trigger waves of Cdk1 activation are responsible for surface contraction waves, ripples in the cell cortex that precede cytokinesis[4,5]. These findings indicate that Cdk1 trigger waves help ensure the spatiotemporal coordination of mitosis in large eggs. Trigger waves may be an important general mechanism for coordinating biochemical events over large distances.

During mitosis, a cell undergoes marked, abrupt reorganization: the chromosomes condense, the Golgi and endoplasmic reticulum fragment, and the dynamics of the microtubules changes. These processes are driven by the activation of the protein kinase Cdk1. In a typical somatic cell, with a cellular radius of the order of 10 μm, it should be relatively easy to achieve a near-synchronous onset of mitosis in all parts of the cell. If Cdk1 were activated abruptly in the middle of the cell (current evidence suggests that Cdk1 is first activated on the centrosomes[6]), then it should take no more than a few seconds for the active complexes to spread by random walk diffusion to all parts of the cell ($t = <d^2>/6D$; assuming the diffusion coefficient $D = 10\ \mu m^2\ s^{-1}$, $t \approx 2$ s). This would be sufficiently fast to account for the observed near-synchronicity of mitotic entry in somatic cells.

However, some eukaryotic cells, notably the well-studied *X. laevis* egg, are much larger; a *Xenopus* egg is approximately 600 μm in radius, which corresponds to a diffusion time on the order of 2 h rather than 2 s. This suggests that mitosis might be a sluggish process in these cells.

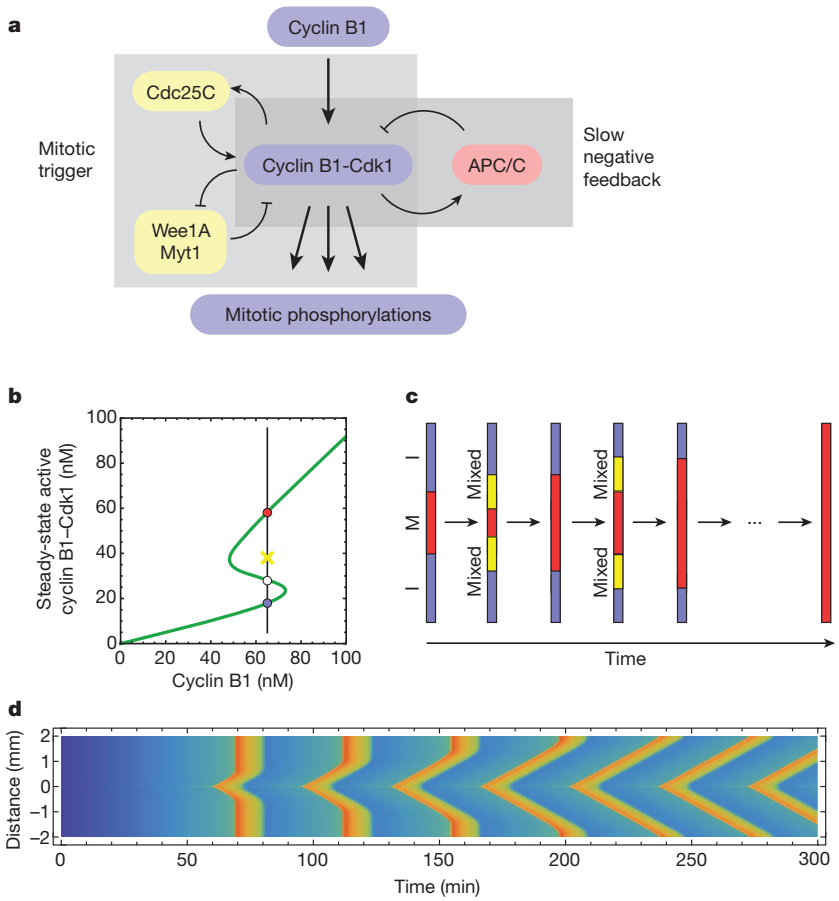

Figure 1 | Trigger waves in Cdk1 activation. **a**, Schematic view of the Cdk1–APC/C circuit. **b**, Modelled steady-state response of Cdk1 to cyclin B1, with parameters on the basis of experimental studies[25,26]. At intermediate concentrations of cyclin, the response is bistable. The stable low (interphase) and high (mitotic) Cdk1 activity steady-states corresponding to one such cyclin concentration (65 nM) are shown as blue and red circles, respectively. The white circle denotes the unstable steady state, and the yellow X denotes an intermediate level of Cdk1 activity that would be attracted to the mitotic (red) steady state. **c**, Schematic view of the propagation of Cdk1 activity up and down a one-dimensional tube through successive rounds of mixing and conversion. I, interphase; M, mitosis. **d**, Modelled propagation of Cdk1 activity in a one-dimensional tube. It is assumed that cyclin B1 is synthesized at a uniform rate everywhere in the tube, but in a 5 μm region in the middle of the tube the concentration of Cdc25C is 50% higher than in the rest of the tube, allowing Cdk1 to become activated earlier. Cyclin B1–Cdk1 activity is denoted by the colour scale (blue is low, red is high). Numerical solution of the partial differential equations used Mathematica 9.0 (Wolfram) as described in the Supplementary Materials. See also Supplementary Fig. 1.

[1]Department of Chemical and Systems Biology, Stanford University School of Medicine, Stanford, California 94305-5174, USA. [2]Department of Biochemistry, Stanford University School of Medicine, Stanford, California 94305-5307, USA.

Actually, the cell cycle is even more rapid in early *Xenopus* embryos than in somatic cells[7]. Moreover, mitotic events occur within minutes of each other in distant parts of the cell. For example, nuclear envelope breakdown, which occurs in the interior of the fertilized egg, takes place only a few minutes before the mitotic surface contraction waves (SCWs; discussed in more detail below) sweep over the cortex of the egg[8]. Thus, some mechanism other than simple diffusion of active Cdk1 must coordinate spatially distant mitotic events.

One possible mechanism is suggested by the systems-level organization of the mitotic trigger circuit, which includes interlinked positive and double-negative feedback loops (Fig. 1a). Circuits such as this can show bistability; indeed, experimental studies in *Xenopus* egg extracts have shown that the response of Cdk1 to non-degradable cyclin B1 is hysteretic, with two alternative stable levels of Cdk1 activity possible at intermediate cyclin B1 concentrations (Fig. 1b)[1,2]. Bistability could, in principle, allow Cdk1 activation to propagate rapidly through trigger waves[3,9–11].

To see why bistability can generate rapidly propagating trigger waves, imagine a long thin tube containing cytoplasm with a uniform concentration of cyclin B1 and Cdk1, and assume that in some region of the tube the cytoplasm is in the mitotic, high Cdk1-activity state (Fig. 1c, red) while the rest of the cytoplasm is in the interphase, low Cdk1-activity state (Fig. 1c, blue). Within some small distance of the interface, the cytoplasm will rapidly mix by diffusion, resulting in an intermediate level of Cdk1 activity. If this activity is above the unstable steady state (Fig. 1b, white point), this slice of cytoplasm will flip to the mitotic state. The process of mixing and conversion repeats, and the mitotic state propagates down the tube at a constant velocity. The propagation speed can be estimated by Luther's formula, $v \approx 2(D/\tau)^{1/2}$, where D is the diffusion coefficient and τ is related to the flipping time for the bistable system[3,12]. If we assume $D = 10\ \mu m^2\ s^{-1}$ and $\tau = 10$–100 s, the expected propagation speed would be 40–120 $\mu m\ min^{-1}$, and Cdk1 activity could propagate from the congressed pronuclei to the animal pole in 2–5 min. This would be fast enough to account for the coordination of nuclear and cortical mitotic events. If Cdk1 activation is followed by APC/C activation and cyclin degradation, a wave of mitotic exit would follow the wave of mitotic entry, and if this is followed by new cyclin synthesis the whole process would repeat.

To explore this idea further, we created a simple partial differential equation (PDE) model of Cdk1 activation and propagation (Supplementary Materials). We assumed that cyclin B1 was synthesized at a uniform, constant rate everywhere in the cytoplasm, and that the mitotic activator Cdc25C was 50% higher in concentration in one 5 μm section of the tube than in the rest of it. This inhomogeneity could represent the centrosome, which, in somatic cells, has a high concentration of Cdc25C[13]. As anticipated, the modelled activation of Cdk1 was found to occur first in this high Cdc25C region, and then to spread linearly up and down the tube, resulting in a V-shaped front of Cdk1 activation in the plot of activity as a function of time and position (Fig. 1d; see also Supplementary Fig. 1). The propagation rate, which is the slope of the diagonal wave fronts, was approximately 60 $\mu m\ min^{-1}$, compatible with the estimates from Luther's formula. Farther from the centrosomal region, cyclin synthesis reached the threshold for Cdk1 activation before the trigger wave arrived, resulting in a vertical front of Cdk1 activity. However, with successive cycles, the trigger waves came to occupy more and more of the tube. These results support the plausibility of trigger waves as a mechanism for allowing Cdk1 activation to spread through an egg in a rapid and orderly manner.

We therefore set out to determine experimentally whether trigger waves do occur, using cycling *X. laevis* egg extracts[14]. De-membranated

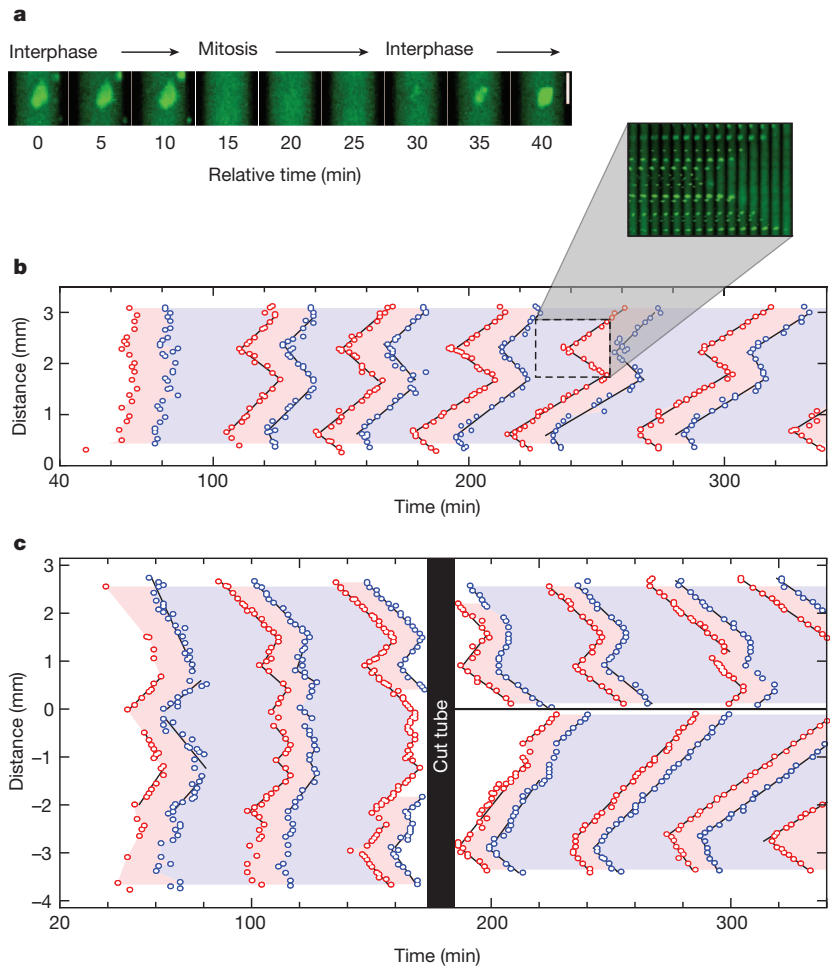

Figure 2 | Rapid, linear propagation of mitotic entry and exit through *Xenopus* cytoplasm. **a**, An example of nuclear envelope breakdown and nuclear envelope reformation in an extract with added sperm chromatin and GFP–NLS. **b**, The timing of mitotic entrance and exit in an approximately 3 mm length of Teflon tubing submerged in mineral oil. Each data point represents the time and position at which an individual nucleus underwent nuclear envelope breakdown (red points) or nuclear envelope reformation (blue points). The pink and blue regions of the plot denote mitosis and interphase, respectively. Time is measured relative to when the extract was warmed to room temperature. The inset shows frames from the video in montage form. **c**, Trigger waves versus phase waves. The tube was cut under mineral oil at 160 min. See also Supplementary Fig. 2.

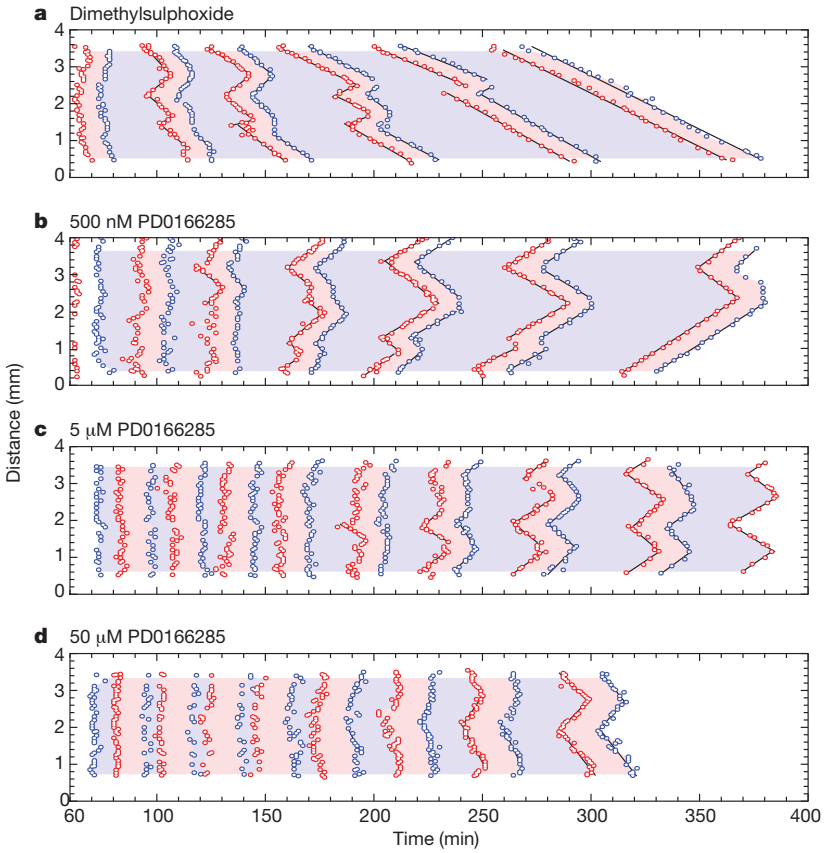

Figure 3 | The Wee1/Myt1 inhibitor PD0166285 accelerates the trigger waves. a–d, Mitotic entrance and exit waves in extracts treated with dimethylsulphoxide or one of three concentrations of PD0166285. See also Supplementary Fig. 3.

sperm chromatin and purified green fluorescent protein (GFP)–nuclear localization signal (NLS) protein were added to the extracts as reporters of mitotic entry. In interphase extracts, the sperm chromatin forms nuclei, complete with nuclear pores that import the GFP–NLS protein. As the cell cycle progresses and the extract enters mitosis, the nuclear envelopes break down and GFP–NLS quickly disperses (Fig. 2a). About 15 min later the nuclei begin to reform (Fig. 2a), indicating the end of mitosis. We loaded extract into a Teflon tube, submerged the tube in mineral oil, and cut the tube into sections 2–3 mm long. These sections were then imaged by time-lapse epifluorescence microscopy. Care was taken to keep the temperature of the tube constant to avoid convective flow. Raw microscopy images were stitched together, and the times and locations of nuclear envelope breakdown and re-formation were recorded.

Supplementary Video 1 and Fig. 2b show the behaviour of a typical cycling extract. The nuclei in the extract initially entered mitosis about 60 min after the extract was warmed to room temperature, and then continued to undergo cycles of interphase and mitosis approximately every 40 min over the next several hours. During the first cycle, the mitoses occurred nearly synchronously, with some apparently stochastic variation in timing from nucleus to nucleus. From the second cycle on, both mitotic entry and mitotic exit swept through the tube in a linear, wave-like fashion (Fig. 2b), with the waves initiating near the same locations during every cycle. Initially the wave speed was $54 \pm 20\ \mu m\ min^{-1}$ (mean ± s.d.), in good agreement with the expected speeds of trigger waves on the basis of either Luther's formula or our PDE simulations (Fig. 1). The waves gradually slowed to about half that speed by the end of the experiment (Fig. 2b and Supplementary Fig. 2). Generally the waves became better organized and spanned longer lengths of the channel as the experiment proceeded (Figs 2b, c and 3a). These findings suggest that waves of mitosis emanating from the earliest or strongest foci eventually dominate the dynamics of the whole system.

In principle, the observed waves could actually be phase waves (also called pseudowaves or kinematic waves[3,15]), which could occur if different parts of the cytoplasm initiated oscillations at different times and this temporal difference was then faithfully maintained in the subsequent waves. To test this possibility, we placed a tube of extract in mineral oil, monitored three cycles of mitotic entry and exit, and then cut the tube into two pieces with a scalpel. As shown in Fig. 2c and Supplementary Video 2, the nuclei on either side of the cut quickly lost coordination, and seemed to follow the rhythm established by the fastest-initiating region of cytoplasm on their side of the cut. This eliminates the possibility that the observed waves are simply phase waves.

If the Cdk1 network generates trigger waves, then changing the dynamics of the feedback loops that regulate Cdk1 should affect wave dynamics. To test this idea, we made use of PD0166285, a small molecule inhibitor of Wee1A and Myt1 (ref. 16). Experiments in bulk extracts showed that inhibition of cyclin B1-induced Cdk1 tyrosine phosphorylation was half-maximal at approximately 1 μM (Supplementary Fig. 3). We treated extracts with 0.5, 5 or 50 μM PD0166285 or just dimethylsulphoxide, and monitored the effects on the timing of mitotic onset and the speed of mitotic propagation.

As shown in Fig. 3 and Supplementary Fig. 3, PD0166285 advanced the onset of mitosis by approximately 30 min and increased the speed of the mitotic waves to as much as $120\ \mu m\ min^{-1}$. Interphase durations were shortened by as much as 50%, and there was an increase in mitotic duration (Supplementary Fig. 3), which emphasizes the importance of Wee1A/Myt1 activation in mitotic exit. At the highest concentrations of PD0166285, waves were not evident until late in the experiment (Fig. 3d). These findings support the hypothesis that the waves of mitotic entry and exit arise from the bistable mitotic trigger.

Finally, we turned to the question of whether the trigger waves seen in extracts also occur in intact fertilized eggs. We considered that waves of Cdk1 activation could be initiated at the centrosome, spread outwards through the cyclin B1–Cdk1 complexes diffusely present throughout the interphase cytoplasm[17], and then cause SCWs when they reach the cortical cytoskeleton. SCWs are waves of pigmentation change at the cell cortex that proceed from the animal pole to the vegetal pole just

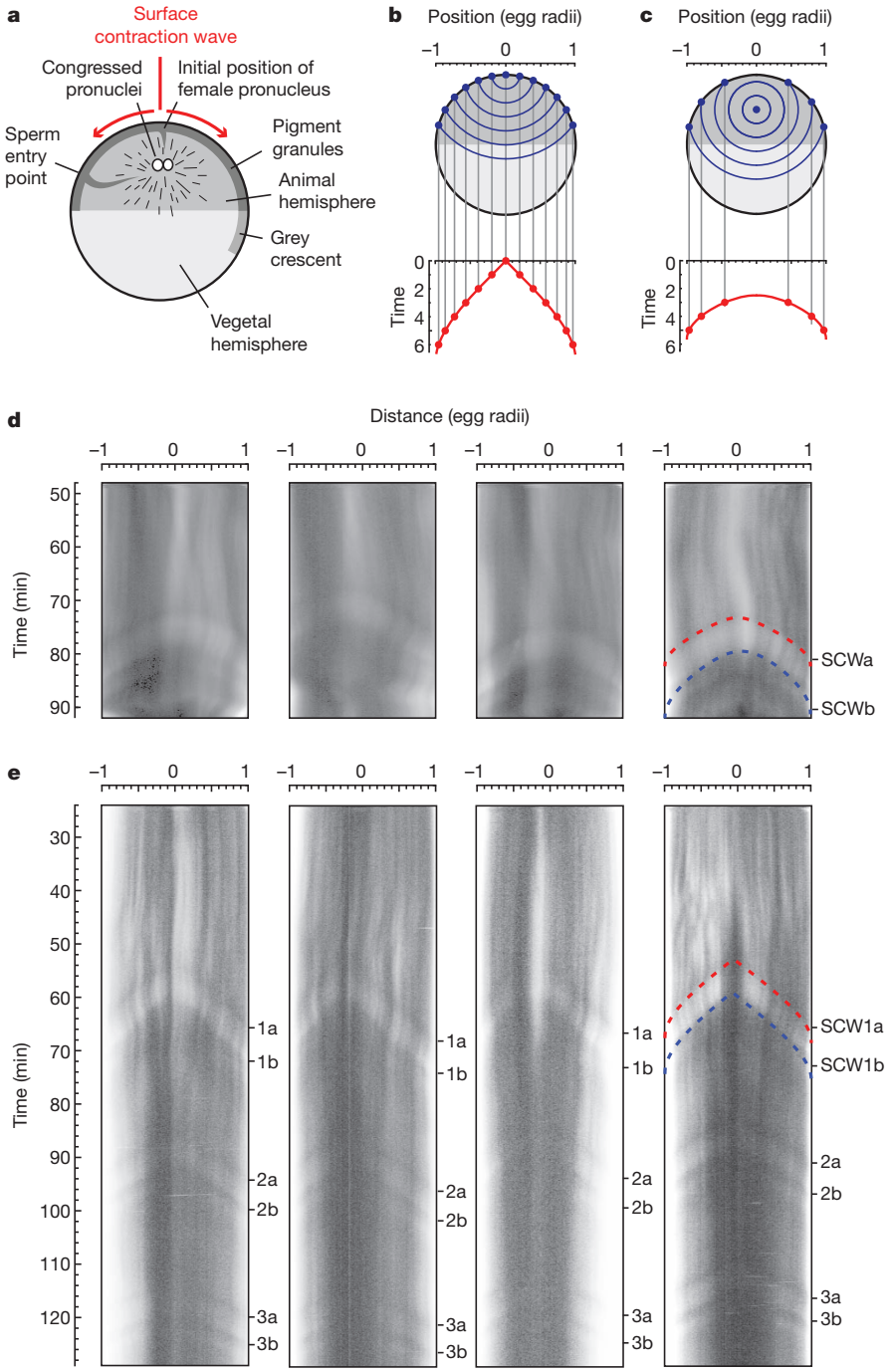

Figure 4 | Surface contraction waves in intact *Xenopus* eggs. **a**, Schematic view of the anatomy of a fertilized egg just before the onset of mitosis (adapted from ref. 27). **b**, **c**, Expected propagation of surface contraction waves if they were due to a spherical wave of Cdk1 activation spreading from a point source. An equation for the spreading of the waves (Supplementary Equation 1) is derived in the Supplementary Materials. Panel **b** assumes the point source is at the animal pole. Panel **c** assumes the point source is halfway between the animal pole and the centre of the cell. **d**, **e**, Kymographs depicting surface contraction waves, indicated by transitions from light to dark or dark to light, in four fertilized eggs (**d**) and four parthenogenetically activated eggs (**e**). The red and blue dashed curves are fits of the experimental data to Supplementary Equation 1. See also Supplementary Fig. 4.

before cytokinesis[4,18,19] (Supplementary Video 3 and Fig. 4a). The first wave (SCWa) is linked to Cdk1 activation, and the second wave (SCWb) requires Cdk1 inactivation[18]. It has been speculated that the change in pigmentation is controlled by the phosphorylation of microtubule associated proteins by Cdk1 (ref. 20).

We derived a formula for the time at which such a constant velocity, spherical wave would reach various points on the surface of the egg as a function of the position of origin of the wave and the wave speed (Supplementary Materials, Supplementary Equation 1 and Supplementary Fig. 4). If the trigger wave were to begin in the middle of the cell, we would expect it to arrive at all points on the cortex simultaneously. If it were to originate from the animal pole, we would expect a plot of the wave's cortical position as a function of time to be V-shaped (Fig. 4b). If it originated in the middle of the animal hemisphere, we would expect the plot to be U-shaped (Fig. 4c).

We then imaged SCWs travelling across the animal hemispheres of fertilized eggs and expressed the data as kymographs (Fig. 4d). The position versus time curves were U-shaped and agreed well with Supplementary Equation 1 (Fig. 4d). By fitting the observed SCWa curves to Supplementary Equation 1, we inferred a trigger wave speed of $66 \pm 17\ \mu m\ min^{-1}$ (mean ± s.d., $n = 4$). This speed is similar to that observed in extracts (Figs 2 and 3). The inferred origin of the waves was at a location 85 ± 5% (mean ± s.d., $n = 4$) up from the vegetal pole on the animal–vegetal axis. This origin is near where the congressed pronuclei reside (Fig. 4a), and the 99% confidence intervals for the location of the origin in each embryo (87–93%, 76–91%, 71–85% and 75–88%) essentially rule out the possibility that the trigger waves originated at the animal pole. The inferred time at which the mitotic trigger wave originated was approximately 70 min after fertilization and 3 ± 1 min (mean ± s.d., $n = 3$) before the beginning of SCWa.

Parthenogenetically activated eggs do not undergo cleavages, but do show a succession of SCWs[5]. Because pronuclear congression does not occur in parthenogenetically activated eggs, it seemed plausible that the spherical mitotic trigger waves considered to give rise to these SCWs might have a different point of origination. As shown in Fig. 4e and Supplementary Video 4, parthenogenetically activated eggs showed a very regular succession of SCWs whose position versus time curves were V-shaped rather than U-shaped. Fitting these curves to Supplementary Equation 1 yielded an inferred wave speed of $58 \pm 3\ \mu m\ min^{-1}$ (mean $\pm$ s.d., $n = 4$) and a point of origination immediately under the animal pole. The 99% confidence intervals for the locations were 99–101%, 98–100%, 99–102% and 98–102% up from the vegetal pole. Thus, the quantitative characteristics of the SCWs both in fertilized and in parthenogenetically activated eggs are consistent with the hypothesis that they occur when trigger waves of Cdk1 activation and inactivation arrive at the cell cortex.

In summary, we have shown through modelling studies that the Cdk1/Wee1A/Cdc25C system could plausibly generate trigger waves of sufficient speed to help spatially coordinate mitosis in the large, fertilized *X. laevis* egg, and have shown experimentally that linear waves of mitotic entry and exit do occur in unstirred cycling *Xenopus* egg extracts and are likely to occur in intact eggs. Note that the early cell cycles of the syncytial *Drosophila* embryo also show mitotic waves. By cycles 10–13, mitosis can been seen to begin at the two poles and spread towards the middle of the embryo, at a rate of approximately 50–$250\ \mu m\ min^{-1}$ (ref. 21). Mitotic waves have also been detected in some mulitnucleate fungi (for example *Stemonitis flavogenita*[22] and *Aspergillus nidulans*[23], but not in *Ashbya gossypii*[24]). We suspect that all of these mitotic waves are essentially the same phenomenon we are observing here.

Random walk diffusion is rapid enough to allow proteins to communicate between different parts of a small cell on a timescale of seconds, and communication in large organisms often takes place by flow. Trigger waves provide another mechanism for communicating rapidly over millimetre to metre distance scales. Trigger waves are the basis for the propagation of action potentials down an axon, for the propagation of calcium waves through excitable cells and tissues, and for cyclic AMP waves in *Dictyostelium discoideum*[9]. Mitotic waves seem to be another example of this phenomenon. The proteins, biochemical processes and timescales involved in action potentials and mitotic waves are different, but the basic systems-level logic is the same. This suggests that trigger waves may be an important general mechanism for communication within tissues, organs and organisms.

METHODS SUMMARY

Time-lapse epifluorescence microscopy of *Xenopus* cycling extracts. Cycling extracts were prepared[14] and, while kept on ice, supplemented with de-membranated sperm chromatin (to approximately 400 per microlitre of extract) and GFP–NLS (to approximately 10 μM). Extracts were then taken off ice and a portion was loaded into Teflon tubing (Cole-Parmer, number YO-06417-72), submerged in mineral oil on a glass slide and cut into 2–3 mm sections.

The tube was imaged at room temperature (22–25 °C) on an inverted epifluorescence microscope (Leica DMI6000 B). Samples from extract not loaded into the tubes were frozen down and later assayed for histone H1 kinase activity.

For studies using PD0166285, extracts were supplemented with a fixed volume of dimethylsulphoxide or inhibitor along with the sperm chromatin and GFP–NLS.

Image analysis. Images of the channels were cropped, stitched together and contrast-adjusted using a custom MATLAB (Mathworks) script. The locations and times at which nuclei underwent envelope breakdown or formation were recorded manually.

Received 28 March; accepted 22 May 2013.
Published online 17 July 2012.

1. Pomerening, J. R., Sontag, E. D. & Ferrell, J. E. Jr. Building a cell cycle oscillator: hysteresis and bistability in the activation of Cdc2. *Nature Cell Biol.* **5,** 346–351 (2003).
2. Sha, W. *et al.* Hysteresis drives cell-cycle transitions in *Xenopus laevis* egg extracts. *Proc. Natl Acad. Sci. USA* **100,** 975–980 (2003).
3. Novak, B. & Tyson, J. J. Modeling the cell division cycle: M-phase trigger, oscillations, and size control. *J. Theor. Biol.* **165,** 101–134 (1993).
4. Hara, K. Cinematographic observation of ''surface contraction waves'' (SCW) during the early cleavage of axolotl eggs. *Wilhelm Roux Arch. Dev. Biol.* **167,** 183–186 (1971).
5. Hara, K., Tydeman, P. & Kirschner, M. A cytoplasmic clock with the same period as the division cycle in *Xenopus* eggs. *Proc. Natl Acad. Sci. USA* **77,** 462–466 (1980).
6. Jackman, M., Lindon, C., Nigg, E. A. & Pines, J. Active cyclin B1-Cdk1 first appears on centrosomes in prophase. *Nature Cell Biol.* **5,** 143–148 (2003).
7. Newport, J. & Kirschner, M. A major developmental transition in early *Xenopus* embryos: I. Characterization and timing of cellular changes at the midblastula stage. *Cell* **30,** 675–686 (1982).
8. Gerhart, J. C. in *Biological Regulation and Development* Vol. 2 (ed. Goldberger, R. F.) 133–316 (Plenum, 1980).
9. Tyson, J. J. & Keener, J. P. Singular perturbation theory of traveling waves in excitable media (a review). *Physica D* **32,** 327–361 (1988).
10. Markevich, N. I., Tsyganov, M. A., Hoek, J. B. & Kholodenko, B. N. Long-range signaling by phosphoprotein waves arising from bistability in protein kinase cascades. *Mol. Syst. Biol.* **2,** 61 (2006).
11. Reynolds, A. R., Tischer, C., Verveer, P. J., Rocks, O. & Bastiaens, P. I. EGFR activation coupled to inhibition of tyrosine phosphatases causes lateral signal propagation. *Nature Cell Biol.* **5,** 447–453 (2003).
12. Luther, R. Raumliche fortplanzung chimischer reaktionen. *Z. Elektrochemie* **12,** 596–600 (1906).
13. Bonnet, J., Coopman, P. & Morris, M. C. Characterization of centrosomal localization and dynamics of Cdc25C phosphatase in mitosis. *Cell Cycle* **7,** 1991–1998 (2008).
14. Murray, A. W. Cell cycle extracts. *Methods Cell Biol.* **36,** 581–605 (1991).
15. Winfree, A. T. Two kinds of wave in an oscillating chemical sollution. *Faraday Symp. Chem. Soc.* **9,** 38–46 (1974).
16. Wang, Y. *et al.* Radiosensitization of p53 mutant cells by PD0166285, a novel G(2) checkpoint abrogator. *Cancer Res.* **61,** 8211–8217 (2001).
17. Nakamura, N., Tokumoto, T., Ueno, S. & Iwao, Y. The cytoskeleton-dependent localization of cdc2/cyclin B in blastomere cortex during *Xenopus* embryonic cell cycle. *Mol. Reprod. Dev.* **72,** 336–345 (2005).
18. Rankin, S. & Kirschner, M. W. The surface contraction waves of *Xenopus* eggs reflect the metachronous cell-cycle state of the cytoplasm. *Curr. Biol.* **7,** 451–454 (1997).
19. Shinagawa, A., Konno, S., Yoshimoto, Y. & Hiramoto, Y. Nuclear involvement in localization of the initiation site of surface contraction waves in *Xenopus* eggs. *Dev. Growth Differ.* **31,** 249–255 (1989).
20. Perez-Mongiovi, D., Chang, P. & Houliston, E. A propagated wave of MPF activation accompanies surface contraction waves at first mitosis in *Xenopus*. *J. Cell Sci.* **111,** 385–393 (1998).
21. Foe, V. E. & Alberts, B. M. Studies of nuclear and cytoplasmic behaviour during the five mitotic cycles that precede gastrulation in *Drosophila* embryogenesis. *J. Cell Sci.* **61,** 31–70 (1983).
22. Haskins, E. F. *Stemonitis flavogenita* (Myxomycetes) – plasmodial phase (aphanoplasmodium). *Film E 2000, Institut Wissenschaftliche Film, Göttingen. Pub. Wiss. Film Sekt. Biol.* **8,** 1–14 (1974).
23. Clutterbuck, A. J. Synchronous nuclear division and septation in *Aspergillus nidulans*. *J. Gen. Microbiol.* **60,** 133–135 (1970).
24. Gladfelter, A. S., Hungerbuehler, A. K. & Philippsen, P. Asynchronous nuclear division cycles in multinucleated cells. *J. Cell Biol.* **172,** 347–362 (2006).
25. Trunnell, N. B., Poon, A. C., Kim, S. Y. & Ferrell, J. E., Jr. Ultrasensitivity in the regulation of Cdc25C by Cdk1. *Mol. Cell* **41,** 263–274 (2011).
26. Yang, Q. & Ferrell, J. E., Jr. The Cdk1-APC/C cell cycle oscillator circuit functions as a time-delayed ultrasensitive switch. *Nature Cell Biol.* **15,** 519–525 (2013).
27. Hausen, P. & Riebesell, M. in *The Early Development of Xenopus laevis: An Atlas of the Histology* plate 12 (Springer, 1991).

Supplementary Information is available in the online version of the paper.

Acknowledgements We thank H. Funabiki and M. Dasso for providing GFP–NLS protein and constructs, E. Sontag and L. Wang for discussions and calculations, T. Tsai for sharing his unpublished data on the effects of PD0166285 on *Xenopus* embryos, Q. Yang for helping to build the ordinary differential equation model upon which our partial differential equation model is based, G. Dey, H. Stone and B. Sullivan for discussions, S. Quake and the Quake laboratory for advice, J. Chen and the Chen laboratory for the use of their microscope and discussions, J. Pomerening for discussions and technical advice, the Stanford Cell Sciences Imaging Facility for technical assistance, and members of the Ferrell laboratory for discussions. This work was supported by grants from the National Institutes of Health (GM046383 and GM077544) and by a National Science Foundation Graduate Research Fellowship and a Lieberman Fellowship (to J.B.C.).

Author Contributions J.B.C. performed experiments and calculations, analysed data and helped write the paper. J.E.F. performed calculations, analysed data and helped write the paper.

Author Information Reprints and permissions information is available at www.nature.com/reprints. The authors declare no competing financial interests. Readers are welcome to comment on the online version of the paper. Correspondence and requests for materials should be addressed to J.B.C. (jbchang@stanford.edu) or J.E.F. (james.ferrell@stanford.edu).